45840

UNITED STATES NAVY
MARINE ENGINEERING LABORATORY
ANNAPOLIS, MARYLAND — 21402

IN REPLY REFER TO:
NP/10310(861)
REPT 68/65

11 MAR 1965

FOR OFFICIAL USE ONLY

FROM: COMMANDING OFFICER AND DIRECTOR
TO: CHIEF, BUREAU OF SHIPS (CODE 634B)

SUBJ: MEL RESEARCH AND DEVELOPMENT PHASE REPORT 68/65; TRANSMITTAL OF

REF: (A) BUSHIPS LTR R007-01-01 SER 634B-579 OF 17 JUL 1963

1. TRANSMITTED HEREWITH IS MEL RESEARCH AND DEVELOPM NT PHASE REPORT 68/65, LOW-CYCLE FATIGUE BEHAVIOR OF INTERNALLY PRESSURIZED BOXES, SUB-PROJECT S-R007-01-01, TASK 0856. THIS IS AN INTERIM REPORT IN THE CONTINUING INVESTIGATION OF THE FATIGUE PROPERTIES OF METALS AND ALLOYS AUTHORIZED IN REFERENCE (A). THE REPORT IS WRITTEN IN THE FORM OF A TECHNICAL PAPER TO BE OFFERED TO ONE OF THE TECHNICAL SOCIETIES FOR POSSIBLE PUBLICATION.

H. V. Nutt

H. V. NUTT
By direction

COPY TO:
(SEE DIST LIST, P II)

FOR OFFICIAL USE ONLY

LOW-CYCLE FATIGUE BEHAVIOR
OF INTERNALLY PRESSURIZED BOXES

ASSIGNMENT 86 108
MEL R&D PHASE REPORT 68/65
SUB-PROJECT S-R007 01 01
TASK 0856
FEBRUARY 1965

BY

M. R. GROSS AND R. E. HEISE, JR.

M. R. Gross
M. R. GROSS

R. E. Heise, Jr.
R. E. HEISE, JR.

APPROVED BY:

W. L. Williams
W. L. WILLIAMS
NAVAL ALLOYS DIVISION

ABSTRACT

One phase of a continuing study of the low-cycle fatigue behavior of metals for deep submergence structural applications involves the validity of simple specimen results when applied to complex structures. As a part of this study, the low-cycle fatigue performance of twelve internally pressurized boxes was investigated. The boxes were constructed from 1-inch thick plate of six materials consisting of three steels, one aluminum alloy, and two titanium alloys.

The boxes were cyclically pressurized at peak nominal stresses up to about 80 percent of the yield strength of the base metal. The results are compared with data previously obtained for simple laboratory specimens. The results of the box tests tend to confirm two general conclusions reached previously from simple specimen tests, that is: (1) increases in low-cycle fatigue strength for a given life are not commensurate with increases in yield strength, and (2) low-cycle fatigue life is closely related to total strain range and appears to be independent of both structural metal and strength level in the life range of 1000 to 30,000 cycles.

TABLE OF CONTENTS

INTRODUCTION

In order to understand, utilize, and defend the vast reaches of the oceans, future submersible vehicles will be expected to descend and operate at increasingly greater ocean depths. Such expectations are consistent with our expanding technology in other areas, such as interplanetary space. Accomplishment in the ocean will require the utilization of materials of higher strength-to-weight ratio, particularly high-strength steels, titanium alloys, and reinforced plastics.

In considering this situation several years ago, it was reasoned that pressure cycles induced by maneuvering deep-submergence vehicles at various depths might possibly limit the life of the pressure hull and certain internal sea-connected equipment. The basis for this reasoning was that structures of high strength-to-weight ratio exposed to sea-water pressure and corrosion would be subjected to a finite number of high stress cycles and, therefore, the useful life of the structures might well be dictated by the resistance of materials to so-called low-cycle fatigue.

For the past several years, the U. S. Navy Maring Engineering Laboratory has been actively engaged in an investigation of the low-cycle fatigue behavior of metallic materials and the consequence of such behavior on the structural integrity of future deep-submergence vehicles. The results of the Laboratory's work on simple specimens, summarized by Gross,[a] indicated that material behavior was predicted

[a]Superscripts refer to similarly numbered entries in Appendix A

differently, depending on the stress or strain parameters being considered. For example, on the basis of total strain, all materials behaved similarly, whereas on the basis of nominal stress, higher-strength materials were superior.

As a result of the above investigation, it became expedient to establish whether the conclusions reached from simple specimens were valid for complex structures. Accordingly, it was decided to investigate the low-cycle fatigue behavior of a structure. It was desirable that the structure be (1) geometrically simple, (2) analytically complex from a stress standpoint, (3) easily tested in the laboratory, and (4) relatively inexpensive. It was also desirable that all of the conditions and factors which were thought to have a significant influence on the fatigue and fracture behavior of a vehicle designed for deep-submergence be present in equal or greater severity in the laboratory structure. The conditions and factors considered to be important were as follows:

- Weldments
- Stress Concentrations
- Cyclic Loads
- Residual Stresses
- Corrosion

From the foregoing considerations, it was concluded that an internally pressurized rectangular box could be constructed and tested such that all of the above conditions and factors would be included. This paper describes the results obtained in the testings of 12 such boxes.

MATERIAL, CONSTRUCTION, AND INSPECTION

Twelve boxes were fabricated from the six different base metals listed in Table 1, using the weld metals indicated in Table 2.

Conditions under which welding was accomplished are also stated in Table 2. The tensile properties shown in Tables 1 and 2 were obtained from specimens removed from low-stressed regions of the boxes after the fatigue tests.

All of the boxes were prepared from wrought plate having a nominal thickness of one inch. The steel and aluminum boxes were fabricated by MEL. The two titanium boxes were fabricated by the U. S. Navy Applied Science Laboratory, Brooklyn, New York.

The first box was constructed from Grade M hull steel using an all-weld-metal corner joint conforming to Class IV, Type C-21 of NAVSHIPS Instruction 250-637-3 of 2 January 1962. The internal dimensions of the box were 5 x 5 x 30 inches. Figure 1 shows the completed box prior to testing, and Item (a), Figure 2, shows the cross section of the box.

Tests on corner-welded boxes showed that cracks initiated at the inside root reinforcement welds and propagated through all-weld metal along a diagonal plane. To provide a path for propagation that could include both weld and base metal, the design of the box was subsequently modified to the J-type joint design (Class IV, Type C-69) shown in Item (b), Figure 2. From early tests it was established that the box was unnecessarily long and that similar results could be obtained by reducing the length of the box to 15 inches. Accordingly, the 5 x 5 x 15-in.* box with the J-joint design shown in Figure 3 became the "standard" box rather early in the program. Nondestructive inspections were made

*Abbreviations used in this text are from the GPO Style Manual, 1959, unless otherwise noted.

on the boxes, both during and after fabrication. The weld beads were inspected as they were laid down, and all cracklike indications were ground out and repaired prior to applying additional weld passes. Upon completion, the boxes were ultrasonically inspected to establish the soundness of the welds and adjacent base metal. The boxes were also ultrasonically inspected after fatigue testing and prior to destructive sectioning to establish the ability of the method to detect and locate cracks. The equipment used in the ultrasonic tests was a Branson Instruments, Incorporated, Model 50B "Sonoray" flaw detector with 2.25-mc, 45° angle probe.

METHOD OF INVESTIGATION

Pressurization System. The structural boxes were cyclically pressurized with the system shown schematically in Figure 4. The system was designed for 10,000 psi maximum pressure, using tap water as the hydraulic fluid. Briefly, operation consisted of (1) completely filling the system with water, (2) pumping against the closed solenoid drain valve until the desired peak pressure was reached, (3) having the preset pressure switch automatically open the drain valve at the peak pressure to drop the pressure to zero, and (4) continuously repeating Steps (2) and (3) under automatic control. The cycling rate of the system was variable, depending upon the volume of liquid to be replaced during each cycle and the capacity of the pump. The system was usually operated at about one cycle per minute.

Measurement System. Anywhere from 12 to 24 resistance-type strain gages (BLH-FAP-25-12) were bonded to the boxes at various external locations to determine the static and dynamic behavior of the boxes. In

addition, a temperature-sensing gage (Ruge Stikon SN-100-3) was attached for monitoring the temperature. Included in the pressurization system was a pressure transducer (Statham Instruments, Model PG731TC-10M-350) for monitoring the system pressure.

On the basis of preliminary static-strain measurements, certain gages were selected for monitoring during the fatigue tests. The selected gages, plus the temperature gage and the pressure transducer, were connected to a transducer input conditioner (B&F Instruments Model 1-202-2AM). The outputs of the conditioner channels were fed into a recording oscillograph (Honeywell Model 1508 Visicorder) for periodic readout.

Stress Calculations. The maximum tensile stress in the pressurized box occurred at the inside corner where the root reinforcement welds were located. The maximum nominal stress at this location was calculated from the following combined stress equation:

$$S_{MAX} = \frac{P A B}{2T (A + B + 2T)} + \frac{P A^2}{2T^2} \quad \text{..............(1)}$$

where: P = peak pressure, psig

A = inside width of box, in.

B = inside length of box, in.

T = plate thickness, in.

The above equation is derived from simple plate theory, assuming uniformly loaded plates with clamped edges having a length-to-width ratio equal to or greater than one. The stress calculations do not include the effects of other factors, such as stress concentrations, residual stresses, etc.

Residual Stress Measurement. Because of the rigidity of the boxes, it was expected that high residual stresses would develop during fabrication. No attempt was made to determine the magnitude and extent of residual stresses in the regions were cracks initiated and propagated. However, estimates of the magnitude of residual surface stresses were obtained from strain-gage readings taken either before and after fabrication or before and after test.

RESULTS OF INVESTIGATION

Static Tests. Prior to the fatigue tests, the boxes were statically pressurized several times to the desired peak internal pressure. While being held at this pressure, the external surface strains were measured at the various longitudinal and transverse strain-gage locations. It was concluded from these measurements that the actual transverse strains agreed quite closely with theoretically predicted strains within the region bounded by ±2 inches of the longitudinal center line. Beyond 2 inches, the edge effects became quite pronounced, and the actual strains were less than the theoretical strains. It was also concluded that plane-strain conditions existed in the central section of the box to within about 5 inches of each end.

Fatigue Tests. Pertinent information about the boxes and the results of the fatigue tests are summarized in Table 3. The maximum nominal peak stresses were calculated from Equation (1) using the cyclic peak pressure and dimensions of the box. The maximum peak strains were obtained by assuming elastic conditions and dividing the maximum peak stresses by the modulus of elasticity, E, and applying a small correction for longitudinal strain. Included in Table 3 are the

percentages of the 0.2-percent yield strength and the corresponding total strain as determined from stress-strain curves of the base metals.

The cycles-to-failure represents the number of peak pressure cycles that the box endured until leakage. The estimated cycles to crack initiation were obtained by monitoring changes in pressure versus strain relationships using the procedures described by Heise.[3] Some of the boxes began to leak slowly, as shown in Figure 5, whereas others developed a large-size crack suddenly. Failure in the latter case was accompanied by a loud "bang." A typical failure of this type is shown in Figure 6.

<u>Ultrasonic Inspection</u>. Ultrasonic inspection of the boxes after fabrication, but prior to fatigue testing, revealed numerous small uninterpretable indications in the regions of the welds for Boxes 10 and 11. It was subsequently established that these indications resulted from lack of penetration between the root pass and root reinforcement bead. The other boxes did not show any significant ultrasonic indications.

Similar inspection after fatigue testing showed that the method was capable of detecting cracks, other than the failure crack, when they existed. The exact number of cracks in a given location, however, and the extent of crack propagation could not be determined by this procedure.

<u>Residual Stresses</u>. The results of the residual stress measurements varied widely, both within and among boxes. No attempt has been made to rationalize the results. It was apparent, however, that peak

transverse residual stresses equal to the yield strength of the base metal were developed in some of the structures. Referring to Table 3, Box 7 is a stress-relieved version of Box 4. The peak residual tensile stresses in Box 4 were observed to be near the yield stress, whereas those in Box 7 were about half the yield stress. It is apparent from the results in Table 3 that the stress-relieving treatment used had no beneficial effect on fatigue life.

Postfailure Examination. Table 4 shows the number and extent of cracks observed in cross sections removed from the boxes at the point of failure after fatigue testing. In some boxes, notably those of steel, cracks initiated and propagated in all four corners. Item (b), Figure 7 is a cross section of this type. In other boxes, principally those of aluminum and titanium, only a single crack initiated and propagated. In all cases, cracks initiated in the inside corners at notches formed by the longitudinal root reinforcement welds.

The final phase of the examination consisted of forcibly opening the failure cracks and examining the fracture surfaces. A description of the failure crack for each of the boxes is given in Figure 8. Except for low-stressed Box 5, the longitudinal crack fronts were quite broad and extended over the plane strain region of the box.. Item (a), Figure 7 is typical.

Fatigue Crack Propagation. Using data in Tables 3 and 4, an average fatigue crack propagation rate can be calculated as follows:

$$\frac{\Delta L}{\Delta N} = \frac{L_F}{N_1 - N_F} \quad \ldots\ldots\ldots\ldots\ldots\ldots\ldots\ldots\ldots\ldots (2)$$

where: $\frac{\Delta L}{\Delta N}$ = average fatigue crack propagation rate

L_F = length (depth of penetration) of failure crack

N_i = estimated cycles to crack initiation

N_F = cycles to failure.

The calculated rates are shown in the right-hand column of Table 3. These values do <u>not</u> indicate the relative crack propagation rates of the materials.

DISCUSSION

In the ensuing discussion, it is important to keep in mind that the assumed stress state and the actual stress state affecting fatigue in a structure may be, and usually are, quite different. It is generally assumed in nominal stress calculations that linear elastic conditions prevail. Under such conditions it is immaterial whether one deals in terms of stress or strain. It is well known, however, that such conditions do not usually prevail in regions of stress intensification where fatigue cracks are most likely to initiate and propagate. This is especially so for the case of low-cycle fatigue. Accordingly, one must recognize that it is unlikely that stress and strain will be linearly related in the region of direct concern.

During the past 10 years much evidence has been developed to support the view that low-cycle fatigue life is a function of strain. One might expect this to be the case, inasmuch as the micromechanisms that are associated with fatigue failure are strain dependent.

Gross[3] and Manson and Hirschberg,[4] and more recently, Wells and Sullivan[5] have shown that low-cycle fatigue specimen results tend to correlate best with the total strain range. The work of Gross has

shown that, in the life range of 100 to 10,000 cycles, low-cycle fatigue crack initiation in test specimens is, within rather narrow probability limits, independent of material and/or strength level but dependent on total strain range. Also, the recent work of Crooker and Lange[1] has shown that low-cycle fatigue crack propagation rate correlates with total strain range, and that the rate appears to be independent of strength level for a given class of material. Different rate-versus-strain relationships have been observed, however, for different materials. In view of the foregoing, it is of interest to examine the results in Table 3 to determine whether the structural boxes follow the same trends as small specimens.

Figure 9 is a log-log plot of total strain range versus number of cycles, which compares the box test results with the smooth specimen relationship obtained previously at MEL for a variety of materials and strength levels. A parallel relationship has been placed through the geometric mean of the box data. There are many differences between the relationship shown for the specimen data and the box data, notably: geometry type of loading, criterion for failure, residual stress, and methods of measuring and calculating total strain. No attempt has been made to take these factors into account at this time. It is apparent, however, that the trend of the box and specimen data is similar. Furthermore, the box data appear to be independent of material and strength level as were the specimen data.

Figure 10 is a log-log plot of equivalent peak stress versus number of cycles to failure. The similarity between the relationships in Figures 9 and 10 appears to be coincidental. It so happens that the

three materials selected for study, i.e., steel, aluminum, and titanium, have almost identical ratios of elastic modulus to density $\left(\frac{E}{\rho}\right)$. Accordingly, the ϵ_T $(\approx \frac{\sigma\ \text{MAX}}{E})$ vs N_F, and $\frac{\sigma\ \text{MAX}}{\rho}$ vs N_F relationships are similar. To demonstrate that strain is the controlling parameter, a test is planned for a box constructed of 70-30 cupronickel alloy, which has a distinctly different $\frac{E}{\rho}$ ratio.

Table 5 compares the fatigue lives of steel boxes in which the peak stress was approximately 80 percent of the yield strength of the base metal. Low-cycle fatigue life appeared as a decreasing function of yield strength. When the yield strength was increased by a factor of 3, the fatigue life decreased by a factor of 10. Comparisons can also be made between Boxes 1 and 5 and between Boxes 4 and 12 in Table 3. The geometry and peak strain of the paired boxes were purposely made nearly identical. In the case of Boxes 1 and 5, there was an increase in the fatigue life of HY-100 steel over the Grade M steel. Not so, however, for Boxes 4 and 12. The lives of both HY-140 steel and HY-100 steel were nearly the same, even though the HY-140 steel was stressed only to 60 percent of its yield strength. In general, the box test results substantiated the observations made on simple specimens, i.e., increases in low-cycle fatigue strength are not commensurate with increases in yield strength of the base metal.

The sudden rupture of the aluminum and the high-interstitial titanium boxes deserve special consideration. The failure of metals by gross fracture may consist of three phases, namely: (1) crack initiation, (2) slow-crack propagation, and (3) fast-crack propagation. If we confine our discussion to the structural boxes, Phases (1) and

(2) are attributable to fatigue unless cracks are present initially, then Phase (1) will already have occurred. In so-called notch-tough materials, Phase (2) will continue until slow leakage occurs, and the net result will not be catastrophic. Phase (3) becomes important when the material tends to behave in a brittle manner.

The fracture-mechanics approach to brittle-fracture problems has shown that, in the presence of a notch, catastrophically fast fractures can occur in high-strength materials at stress levels well below the yield strength. It has also been demonstrated that there is a critical crack size that high-strength materials can tolerate which is dependent upon their plane-strain fracture toughness. Beyond this critical size, cracks become self-propagating at low-stress levels, and catastrophic failure can occur.

The critical crack size aspect of fracture mechanics was readily evident in the failure of Box 8 (Ti-A70). Examination of the fracture revealed a slow crack propagation phase (see Item (b), Figure 6) followed by rapid propagation which cracked the box along almost its entire length. Although the failures of Boxes 6 (Al-6061) and 11 (Ti-6Al-4V) were somewhat similar, no distinct areas of slow and fast crack propagation could be observed. A low-interstitial, high-toughness, titanium-alloy box is to be tested in the near future to provide additional information on the mechanism of final failure.

HY-100 steel is a notch-tough material, and experience has shown that failure will be of the slow leakage type. Accordingly, the sudden rupture of Box 2 requires some explanation. As can be observed in Figure 8, the final fracture path was along a plane of maximum shear.

Presumably, there was a weak junction between adjacent surface weld beads, and shear failure occurred suddenly along this junction.

Figure 11 is a log-log plot of the average crack propagation rate versus total strain range data in Table 3. Included in Figure 11 is the relationship obtained by Crooker and Lange[1] from specimen tests. The relationship was purposely positioned so that it passed through the geometric mean of the data. The agreement between the data and the relationship is surprising considering the uncertainties of the method used to determine the average crack propagation rates for the boxes.

It should be recognized in Figure 11 that what appear to be minor deviations from Crooker and Lange's relationship do, in fact, represent rather large differences in crack propagation rate. For example, the calculated crack propagation rate for Box 9 is about twice that which would have been predicted by the relationship. In general, it is concluded from the data in Figure 11 that under the conditions of the test, there are no significant differences in crack propagation rates between the various materials.

In designing the structural box test, the intent was to introduce as many important variables as possible in order to establish their gross effect. It was deemed important, however, that the joining procedures used in construction meet at least the minimum requirements of acceptable standards. It is apparent from the results that the low-cycle fatigue life of the box structures was more dependent on design and fabrication than on material. Substantial improvements in life can be brought about by delaying crack initiation and/or slowing down crack propagation. Basically, this can be accomplished by (1) mechanically

removing sharp fillets, notches, and cracks in critical areas, (2) removing undesirable residual stresses by thermal or mechanical stress relief, and (3) introducing desirable residual stresses by mechanical cold working techniques.

CONCLUSIONS

The results of the low-cycle fatigue tests of structural boxes cyclically pressurized with fresh water tend to confirm two general conclusions reached previously from tests of simple specimens. These are:

- Increases in low-cycle fatigue strength for a given life are not commensurate with increases in yield strength.
- Low-cycle fatigue life is closely related to total strain range, and on this basis appears to be independent of both the structural metal and strength level in the life range of 1000 to 30,000 cycles.

It is concluded from the box test results that:

- Low-cycle fatigue life of a complex structure can be far more sensitive to design and fabrication than to the materials from which it is made.
- Final failure of high strength-to-weight structures subjected to low-cycle fatigue can be sudden and extensive if the material of construction has low notch toughness.
- Fatigue crack propagation rate is (1) strain dependent and (2) independent of material of construction.

FUTURE PLANS

Short-range plans include (1) comparative tests on maraging steels and newly developed notch-tough titanium alloys, and

(2) definitive tests to establish the importance of various factors, especially corrosion. The long-range effort will be directed toward a synthesis of the box results. Each of the important factors affecting low-cycle fatigue failure will be studied and combined in an effort to improve the engineer's ability to predict the final results.

Table 1

Base Metal Chemical Composition and Mechanical Properties

	Base Metal					
	Grade M Hull Steel	HY-100 Hull Steel	HY-140 Hull Steel	Aluminum Alloy 6061-T65H	Titanium Alloy A70(1)	Titanium Alloy 6Al-4V[1]
Nominal Chemical Composition, %						
C	Max 0.28	0.17	0.10			
Mn	0.75	0.30	0.75			
Ni	Max 0.25	3.00	5.10			
Cr		1.40	0.55	0.25		
Mo		0.40	0.55			
V			0.07			4.0
Al				Bal		6.0
Ti					≈100	Bal
Fe	Bal	Bal	Bal		N_2/0.007	N_2/0.0064
Si	0.25	0.25	0.30	0.6	H_2/0.0073	N_2/0.0039
Cu	Max 0.35			0.25	O_2/0.317	O_2/0.156
Mg				1.0		
Mechanical Properties						
Yield Strength (0.2%), psi	44900	109000	143500	40000	76300	127900
Tensile Strength, psi	70400	123700	151000	43000	99400	134400
Elongation in 2 in., %	33	21	21	15	25	12
Reduction of Area, %	54	70	68	38	49	28
Modulus of Elasticity, psi	30×10^6	30×10^6	30×10^6	10×10^6	15.5×10^6	16.5×10^6

[1]Note high-interstitial content

Table 2

Base Metal - Weld Metal Combinations Used in Preparing Test Boxes

	Base Metal					
	Grade M Hull Steel	HY-100 Hull Steel	HY-140 Hull Steel	Aluminum Alloy 6061-T65H	Titanium Alloy A70	Titanium Alloy 6Al-4V
Filler Metal	AWS-E6014	Type - E11018	Airco HT5256-C	Type 4043	Ti-55A	Ti-6Al-4V
Process	Manual Metal Arc	Manual Metal Arc	MIG	MIG	Short Circuit MIG	Short Circuit MIG
Gas Shield	None	None	98% A - 2% O_2	75% He - 25% A	75% A- 25% He + Argon Trailing Shield	75% A- 25% He + Argon Trailing Shield
Preheat, F	None	150-250	150	None	100-200	150-200
Max Interpass Temp, F	200	300	150	200	100-200	150-200
Tensile Properties of Weld Metal						
Yield Strength (0.2%), psi	66600	99800	137400	24600	65800	130000
Tensile Strength, psi	78400	112000	146600	34000	80600	144300
Elongation in 2 in. %	24	25	19	12	22	8
Reduction of Area, %	42	69	68	21	41	12

Table 3

Summary of Results

Box No.	1	2	3	4	5A	5B	6	7	8	9	10	11	12
Base Metal	Grade M	HY-100	HY-100	HY-100	HY-100	HY-100	Al-6061-T65H	HY-100	Ti-A70	Al-6061-T65H	HY-140	Ti-6Al-4V	HY-140
Type of Weld	Corner	Corner	J	J	Corner	Corner	J	J	J	J	J	J	J
Condition of Box	As welded	As welded	As welded	As welded	As welded	As welded	Retreated[1]	SR[2]	As welded	Retreated[1]	As welded	As welded	As welded
Nominal Inside Dimensions, in.	5 x 5 x 30	5 x 5 x 30	5 x 5 x 30	5 x 5 x 15	5 x 5 x 30	5 x 5 x 30	5 x 5 x 15	5 x 5 x 15	5 x 5 x 7 1/2	5 x 5 x 15	5 x 5 x 15	5 x 5 x 15	5 x 5 x 15
Plate (Wall) Thickness, in.	0.970	0.924	0.918	0.946	0.940	0.940	0.995	0.905	0.96-1.04	0.994	0.981	0.893	0.922
Cyclic Peak Pressure, psig	2550	6000	5050	5450	2370	3990	2250	5350	3700	1530	7750	3750	5200
Nominal Stress and Strain Values													
Maximum Peak Stress, σ_{MAX}, psi	39,200	101,000	86,000	86,100	38,600	65,100	32,300	91,800	53,800	22,000	114,800	65,900	86,200
Percent of 0.2% Yield Strength	86.2	92.7	78.9	79.0	35.5	59.7	80.9	84.3	70.5	55.0	80.0	53.2	60.0
Maximum Peak Strain e_{MAX}, in/in	.00128	.00330	.00281	.00281	.00126	.00212	.00316	.00300	.00338	.00214	.00374	.00390	.00281
Percent of Total Strain to 0.2% Yield Strain	37.7	56.9	48.4	48.4	21.7	36.5	53.5	51.7	49.0	36.3	55.0	40.6	41.3
Estimated Cycles to Crack Initiation N_i	15,000	1500	2000	1500	70,000	-	1500	1700	1200	2500	(4)	(4)	1400
Cycles to Failure N_F	26,400	7100	9600	8300	100,000+	3000	6400	6200	5500	10,500	2500	1900	8600
Type of Failure	Slow leak	Sudden rupture	Slow leak	Slow leak	None[3]	Slow leak	Sudden rupture	Slow leak	Sudden rupture	Slow leak	Slow leak	Sudden rupture	Slow leak
Average Crack Propagation Rate, μin per cycle	104	223	165	184	25	125	255	250	232	156	500	725	156

[1] Solution treated and aged after welding longitudinal edges.
[2] Stress relieved. Heated to 950 F, held 2 hr, furnace cooled.
[3] Test stopped at 100,000 cycles. Pressure raised to 3990 psig and test continued to failure.
[4] Ultrasonic crack indications present prior to test. Examination of fracture showed lack of fusion at root pass.

Table 4
Number and Length of Fatigue Cracks in Cross Sections
[Corners in Rotation Starting with Failure (F)
Crack as No. 1; Crack Length in Inches].

Box No.	Material	Corner 1		Corner 2		Corner 3		Corner 4		Total No.
		No.	Length	No.	Length	No.	Length	No.	Length	
1	Grade M	F 1	1 3/16 1/8	1	1/4	1 1	1/8 3/8	1	5/8	6
2	HY-100	F	1 1/4	1 1	1/8 5/8	1	13/16	2	5/16	6
3	HY-100	F 1	1 1/4 5/8	1 1	1/8 1/2	1 1	5/16 11/16	1 1	3/16 1/2	7
4	HY-100	F 1	1 1/4 1/2	1 1	1/8 7/16	1 1	1/8 3/4	1 1	1/8 9/16	8
5	HY-100	F	1 1/8 [1]	-	-	-	-	-	-	1
6	AL-6061	F	1 1/[illegible]	1	5/8	-	-	-	-	2
7	HY-100	F	1 1/8	1 1	5/16 3/4	1 1	1/4 3/4	1	7/8	6
8	Ti-A70	F	1 1/4 [2]	-	-	-	-	-	-	1
9	AL-6061	F	1 1/4	-	-	-	-	-	-	1
10	HY-140	F	1 1/4	1	1/2	1	5/16	-	-	3
11	Ti-6Al-4V	F	1 3/8	-	-	-	-	-	-	1
12	HY-140	F 1	1 1/8 1/4	1	1/2	1	5/8	1	9/16	5

[1] Box tested at two stress levels (see Table 3).
Length of failure crack first level - 3/4 inch, 2nd level - 3/8 inch, total - 1 1/8 inches.
[2] Length of fatigue portion of crack - 1 inch.

Table 5

Comparison of Steel Boxes Having $\sigma_{MAX} \approx 0.8\ \sigma_{YS}$

Box No.	Material	$\sigma_{YS\ HY}/\sigma_{YS\ M}$	N_F
1	Grade M	1.0	26400
3	HY-100	2.[illegible]	9600
4	HY-100	2.4	8300
10	HY-140	3.2	2500

USN
MARINE ENGINEERING LABORATORY

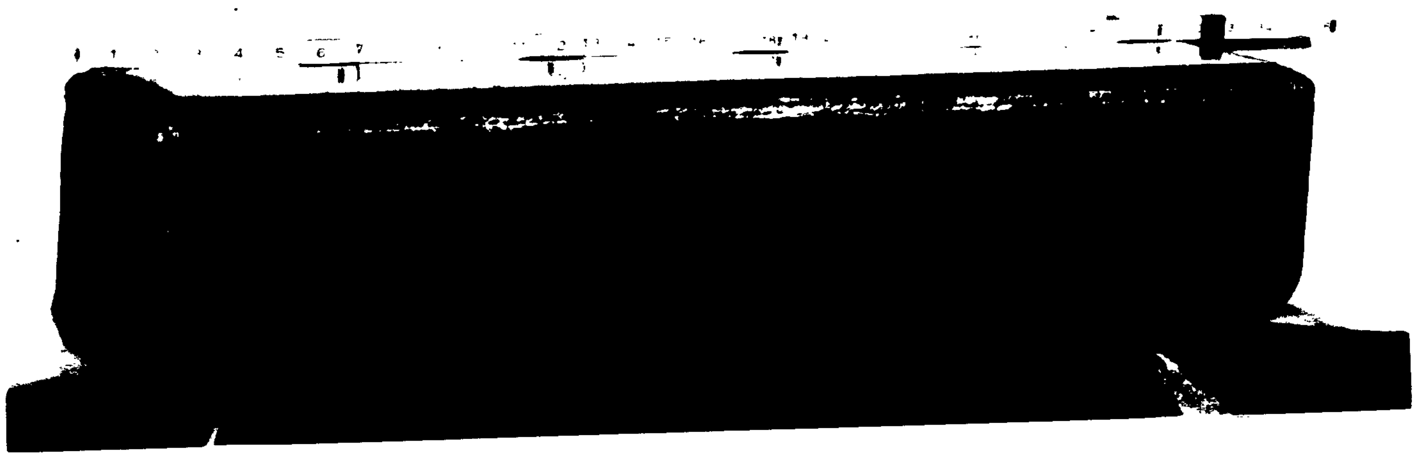

Figure 1

Corner Weld Box Prior to Test

USN
MARINE ENGINEERING LABORATORY

Item (a) - Class IV,
Type C-21 Corner Weld

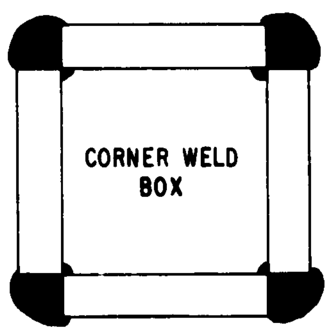

Item (b) - Class IV,
Type C-69 Corner Weld

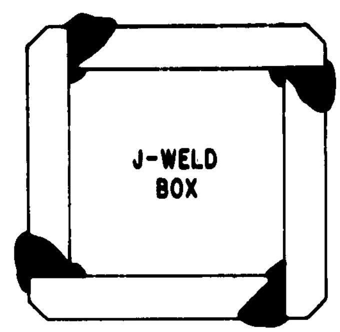

Figure 2
Cross Sections of Structural Boxes

USN
MARINE ENGINEERING LABORATORY

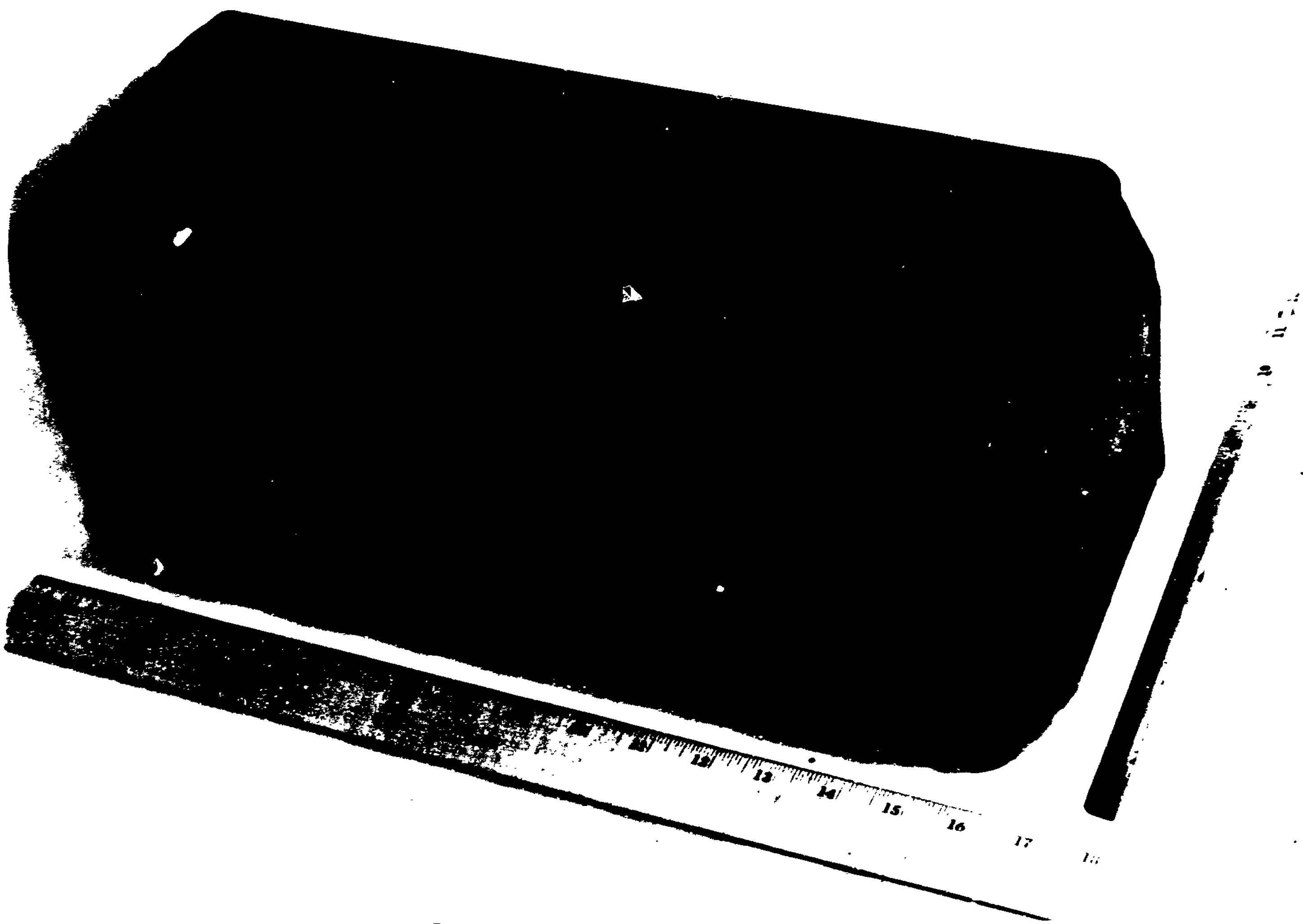

Figure 3 - J-Weld Box Prior to Test

USN
MARINE ENGINEERING LABORATORY

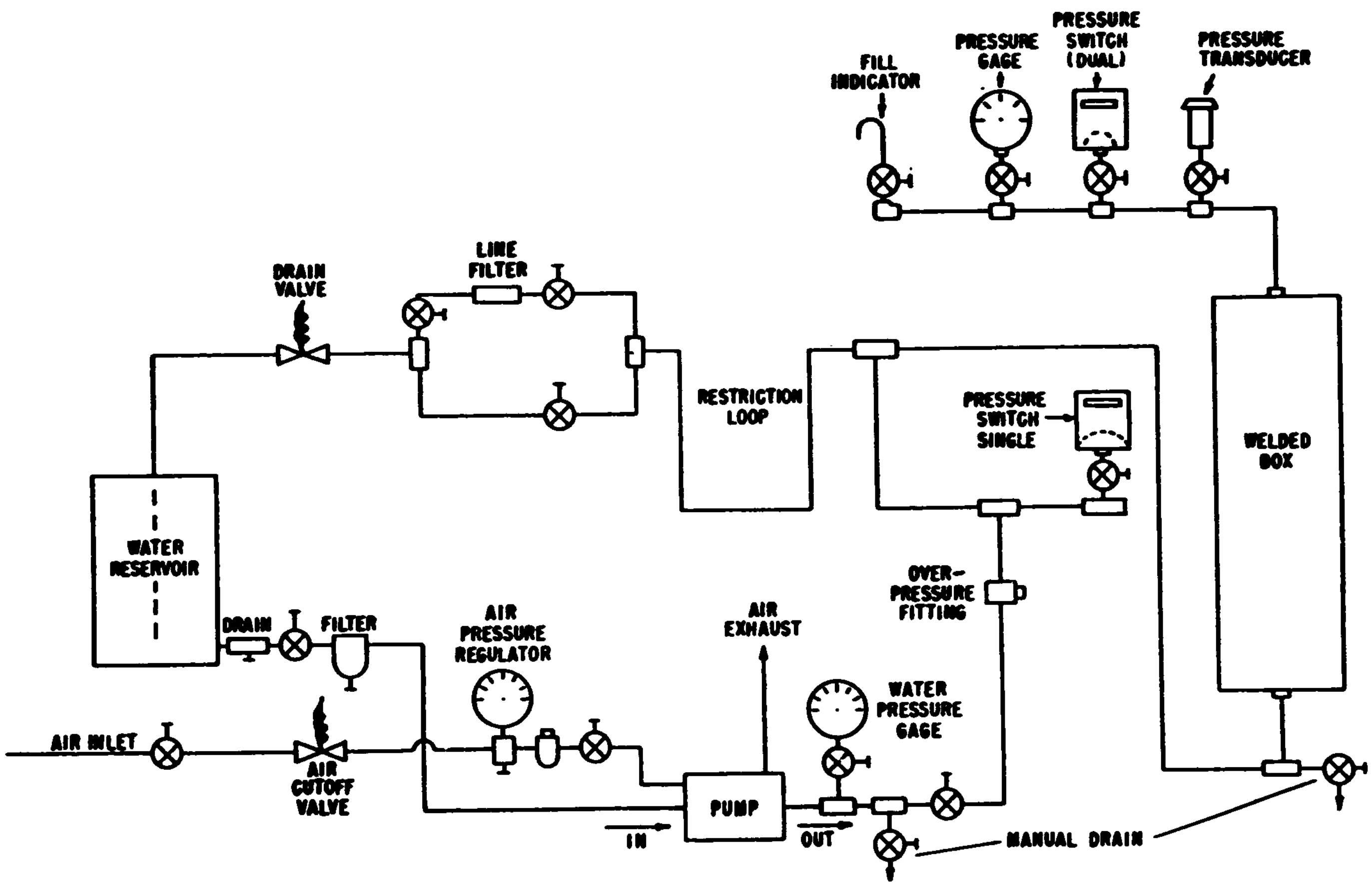

Figure 4

Pressurization System for Structural Box Fatigue Tests

USN
MARINE ENGINEERING LABORATORY

Figure 5

Typical Slow Leak (Box 9)

USN MARINE ENGINEERING LABORATORY

Item (a) - Full-Length Longitudinal Crack in Base Metal

Item (b) - Fracture Appearance

Figure 6 - Sudden Rupture of Box 8

USN MARINE ENGINEERING LABORATORY

Item (a) - Longitudinal Fracture Surface (Portion Removed for Cross Section Below)

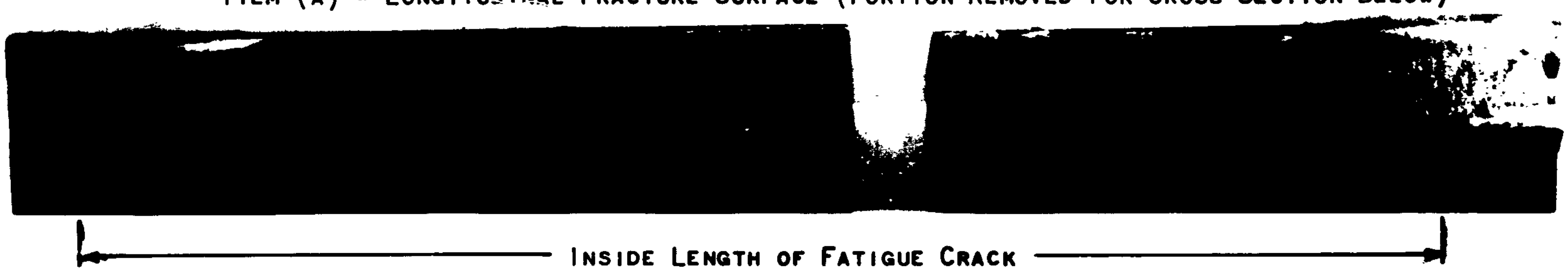

Item (b) - Etched Cross Section (Arrows Point to Cracks)

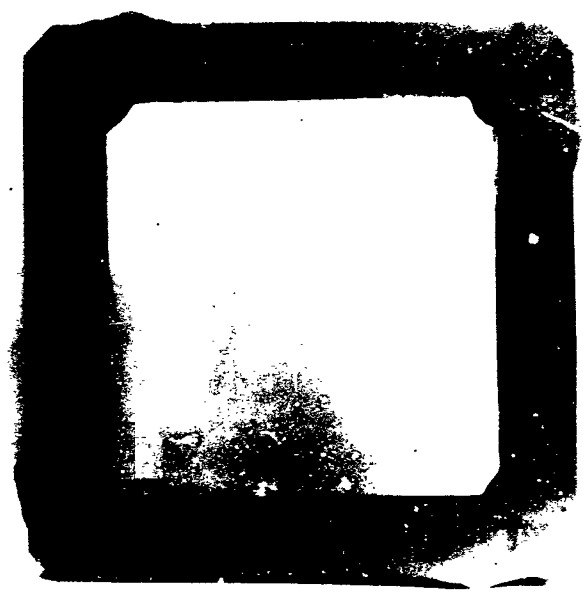

Figure 7 - Fracture Surface and Cross Section of Box 12

R. No.	MATERIAL	TRANSVERSE SECTION OF THROUGH CRACK	LONGITUDINAL SURFACE OF THROUGH CRACK	REMARKS
	GRADE M		L_E = LEAK L_I = 28"	FATIGUE CRACK PROPAGATION TO SLOW LEAK IN WELD. SHOWED EVIDENCE OF MANY CRACK INITIATIONS.
2	HY-100		L_E = 9-10" L_I = 28"	FATIGUE CRACK PROPAGATION PARTIALLY THROUGH FOLLOWED BY SHEAR RUPTURE IN WELD.
3	HY-100		L_E = LEAK L_I = 25"	FATIGUE CRACK PROPAGATION TO SLOW LEAK.
4	HY-100		L_E = LEAK L_I = 12"	FATIGUE CRACK PROPAGATION TO SLOW LEAK.
5	HY-100	3/4" 3/8"	L_E = LEAK L_I = 5" (5A) L_I = 7" (5B)	TWO-STAGE TEST (SEE TABLE 4). SHOWED SELECTIVE INITIATION. FATIGUE CRACK PROPAGATION TO SLOW LEAK.
6	AL-6061		L_E = 7" L_I = 9"	FATIGUE CRACK PROPAGATION PARTIALLY THROUGH FOLLOWED BY FAST FRACTURE IN WELD METAL.
7	HY-100		L_E = LEAK L_I = 11"	FATIGUE CRACK PROPAGATION TO LEAK IN BASE METAL. BUILDUP OF PLASTICALLY DEFORMED METAL ALONG EXTERIOR ADJACENT TO CRACK.
8	TI-A70		L_E = 7" L_I = 7" L_I FATIGUE = 5"	FATIGUE CRACK PROPAGATION PARTIALLY THROUGH BASE METAL FOLLOWED BY FAST FRACTURE ALONG FULL LENGTH.
9	AL-6061		L_E = 1/8" L_I = 10"	FATIGUE CRACK PROPAGATION TO MULTI-HOLE LEAK AT BASE-WELD METAL BOUNDARY.
10	HY-140		L_E = LEAK L_I = 10 1/2"	FATIGUE CRACK PROPAGATION TO LEAK AT BASE-WELD METAL BOUNDARY. LACK OF FUSION BENEATH ROOT PASS.
11	TI-6AL-2V		L_E = 9-10" L_I = 14-15"	AREA OF FATIGUE CRACK PROPAGATION NOT EVIDENT. SUDDEN RUPTURE FOR EXTENDED LENGTH. LACK OF FUSION BENEATH ROOT PASS. NOTE TRIPLE PASS REINFORCEMENT WELD.
12	HY-140		L_E = LEAK L_I = 11"	FATIGUE CRACK PROPAGATION TO LEAK IN BASE METAL. BUILDUP OF PLASTICALLY DEFORMED METAL NEAR LEAK.

NOTE: L_E = LENGTH OF EXTERNAL CRACK; L_I = LENGTH OF INTERNAL CRACK.

FIGURE 8 - DESCRIPTION OF CRACKS LEADING TO FINAL FAILURE

USN
MARINE ENGINEERING LABORATORY

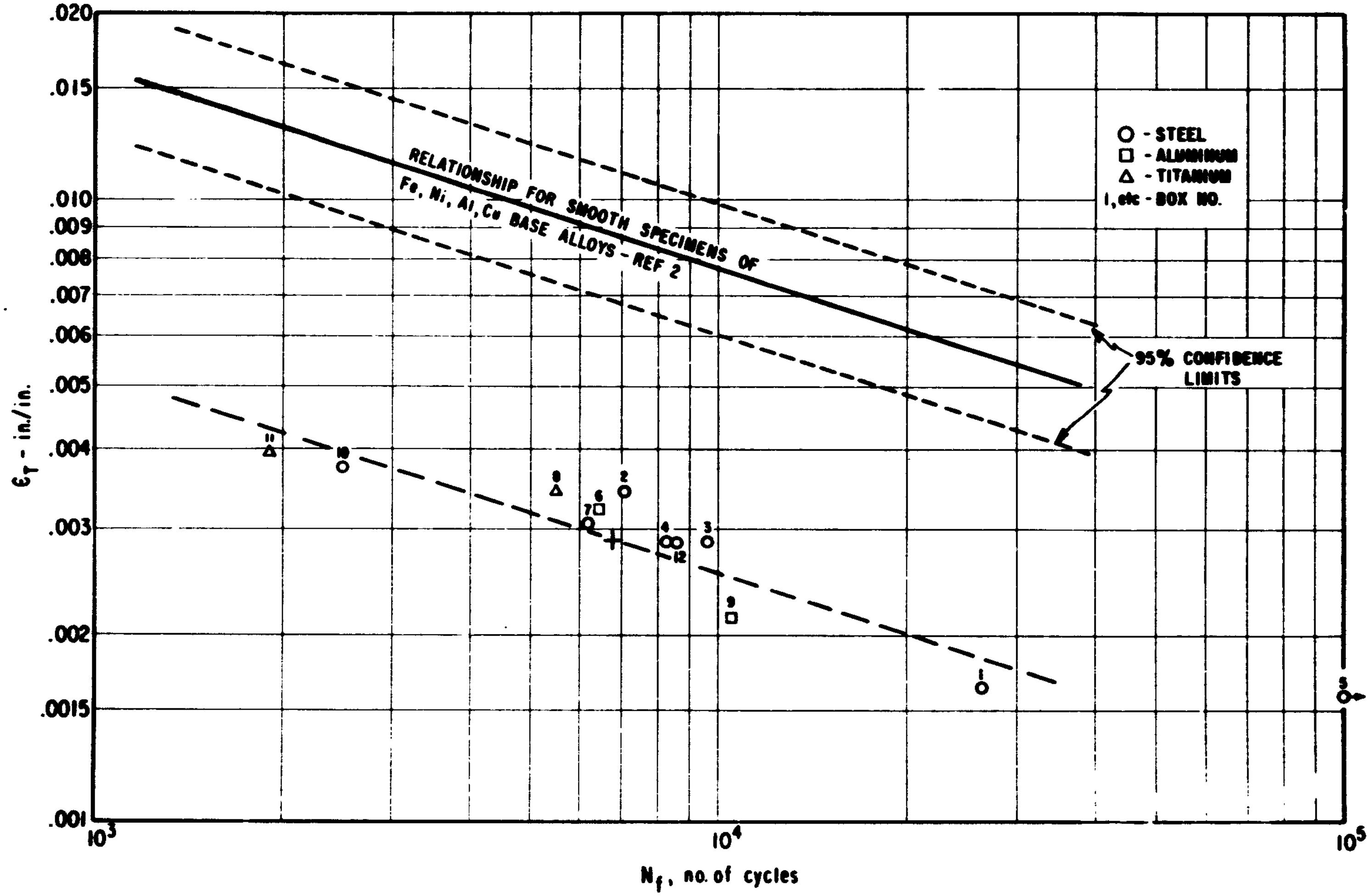

FIGURE 9 - TOTAL STRAIN RANGE (ϵ_T) VS NUMBER OF CYCLES TO FAILURE (N_F)

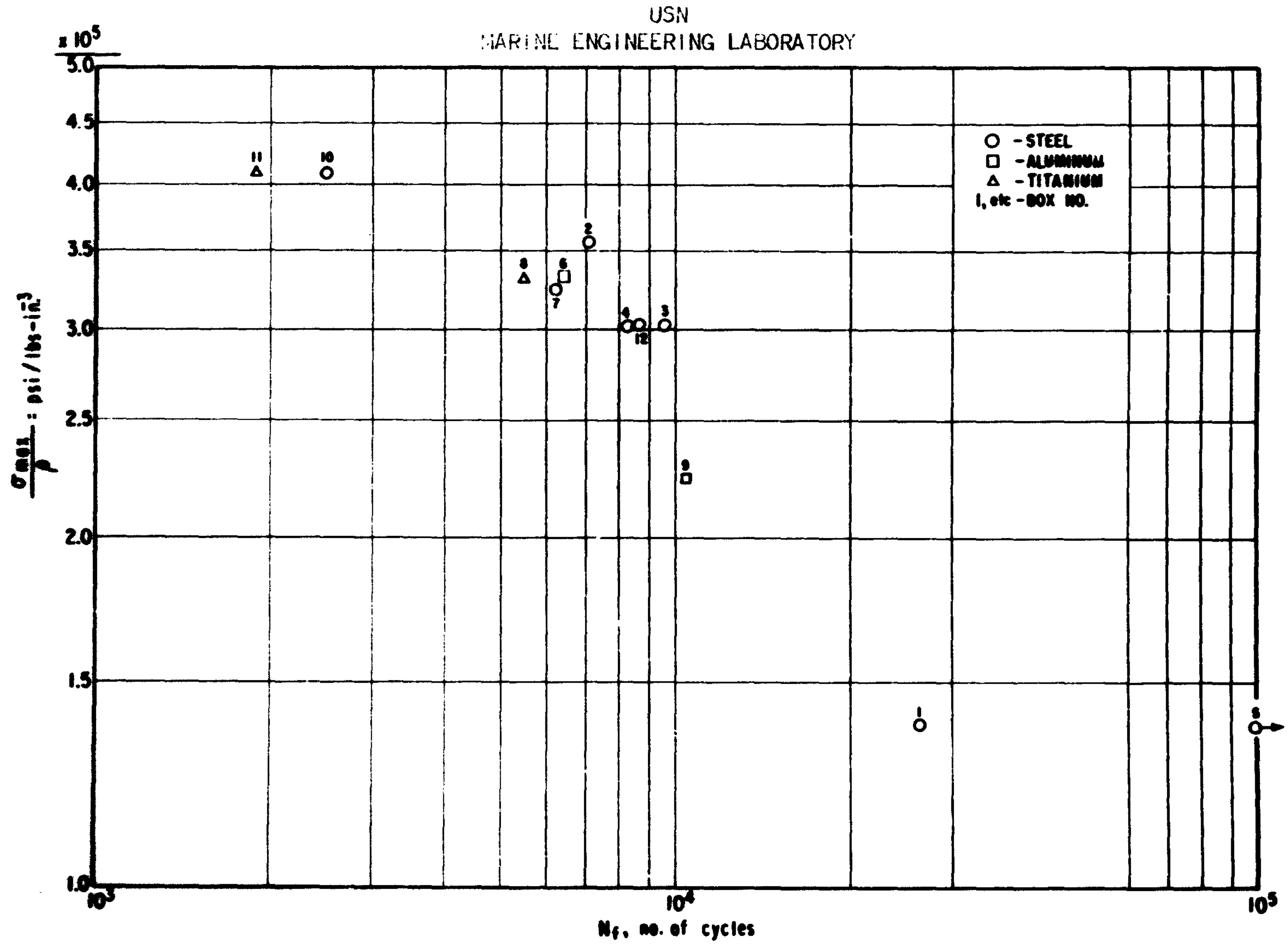

Figure 10 - Equivalent Peak Stress $\left(\frac{\sigma\ MAX}{\rho}\right)$ vs Number of Cycles to Failure (N_F)

USN
MARINE ENGINEERING LABORATORY

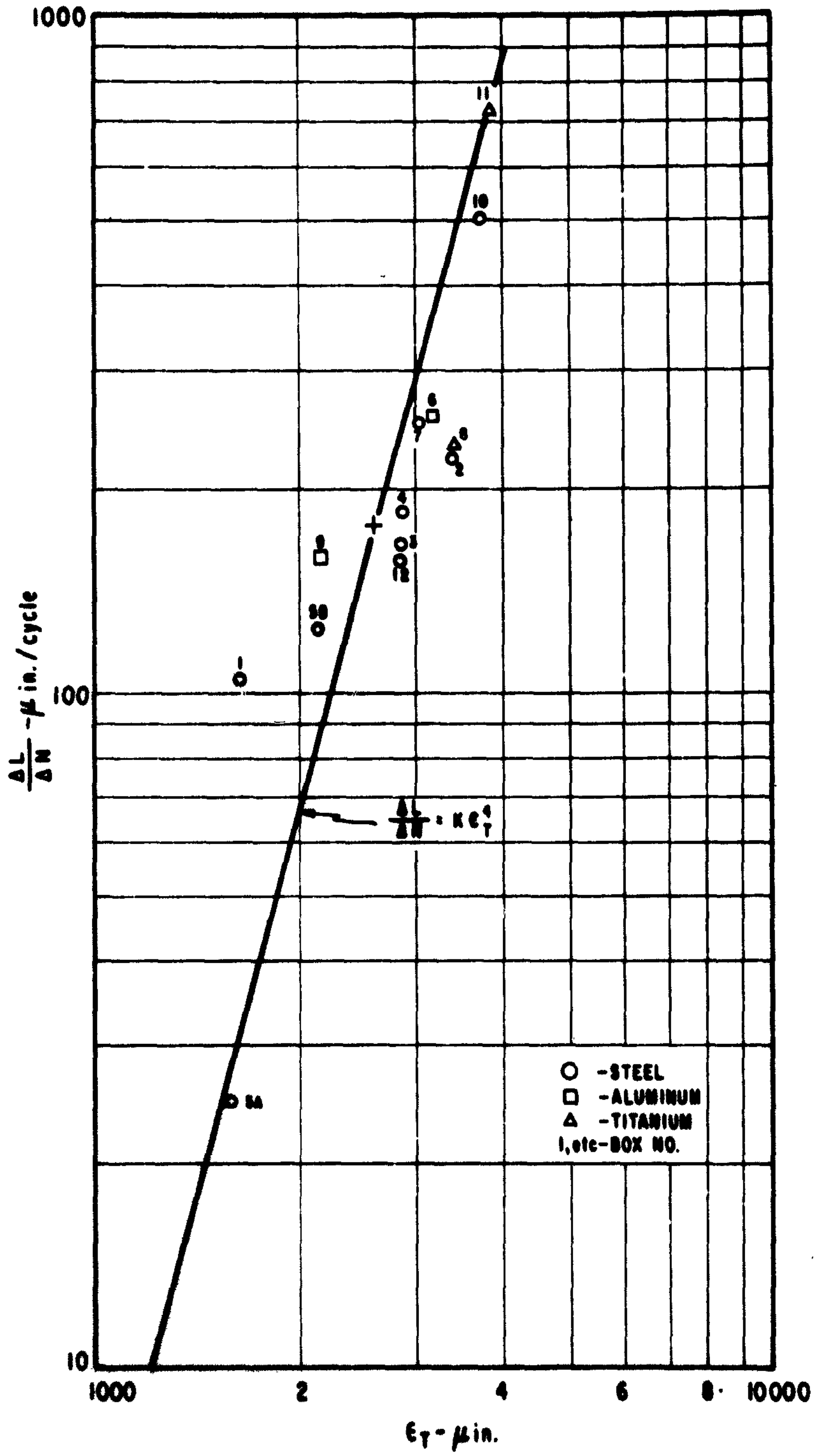

Figure 11

Average Crack Propagation Rate $\left(\frac{\Delta L}{\Delta N}\right)$ vs Total Nominal Strain Range (ϵ_T)

Appendix A

Bibliography

1 - Crooker, T. W., and Lange, E. A., "Low-Cycle Fatigue and Crack Growth Rates in Quenched and Tempered Steels at Various Strength Levels," NRL Rept 6086, Jan 1964

2 - Gross, M. R., "Low-Cycle Fatigue of Materials for Submarine Construction," Naval Engineers Jour. Vol. 75, No. 4, Oct 1963

3 - Heise, R. E., Jr., "Low-Cycle Fatigue Crack Indications by Strain Gages Operating in Elastic Strain Fields," MEL Rept 86 108D, May 1964

4 - Manson, S. S., and Hirschberg, M. H., "Fatigue Behavior in Strain Cycling in the Low- and Intermediate-Cycle Range," Fatigue - An Interdisciplinary Approach, Syracuse University Press, 1964

5 - Wells, C. H., and Sullivan, C. P., "The Low-Cycle Fatigue Characteristics of a Nickel-Base Superalloy at Room Temperature," Trans. ASM, Vol. 57, No. 4, Dec 1964

Navy Marine Engineering Laboratory.
Report 68/65
LOW-CYCLE FATIGUE BEHAVIOR OF INTERNALLY PRESSURIZED BOXES, by M. R. Gross and R. E. Heise, Jr. February 1965. 32 pp. Figs.
UNCLASSIFIED

One phase of a continuing study of the low-cycle fatigue behavior of metals for deep submergence structural applications involves the validity of simple specimen results when applied to complex structures. As a part of this study, the low-cycle fatigue performance of twelve
(over)

1. Steel - Fatigue
2. Aluminum Alloy-Fatigue
3. Titanium Alloy-Fatigue
I. Gross, M. R.
II. Heise, R.E., Jr.
III. Title
IV. Title: Fatigue..

UNCLASSIFIED

internally pressurized boxes was investigated. The boxes were constructed from 1-inch thick plate of six materials consisting of three steels, one aluminum alloy, and two titanium alloys. The boxes were cyclically pressurized at peak nominal stresses up to about 80 percent of the yield strength of the base metal. The results are compared with data previously obtained for simple laboratory specimens. The results of the box tests tend to confirm two general conclusions reached previously from simple specimen tests, that is: (1) increases in low-cycle fatigue strength for a given life are not commensurate with increases in yield strength, and (2) low-cycle fatigue life is closely related to total strain range and appears to be independent of both structural metal and strength level in the life range of 1000 to 30,000 cycles.

Navy Marine Engineering Laboratory.
Report 68/65
LOW-CYCLE FATIGUE BEHAVIOR OF INTERNALLY PRESSURIZED BOXES, by M. R. Gross and R. E. Heise, Jr. February 1965. 32 pp. Figs
UNCLASSIFIED

One phase of a continuing study of the low-cycle fatigue behavior of metals for deep submergence structural applications involves the validity of simple specimen results when applied to complex structures. As a part of this study, the low-cycle fatigue performance of twelve
(over)

1. Steel - Fatigue
2. Aluminum Alloy-Fatigue
3. Titanium Alloy-Fatigue
I. Gross, M. R.
II. Heise, R.E., Jr.
III. Title
IV. Title: Fatigue..

UNCLASSIFIED

internally pressurized boxes was investigated. The boxes were constructed from 1-inch thick plate of six materials consisting of three steels, one aluminum alloy, and two titanium alloys. The boxes were cyclically pressurized at peak nominal stresses up to about 80 percent of the yield strength of the base metal. The results are compared with data previously obtained for simple laboratory specimens. The results of the box tests tend to confirm two general conclusions reached previously from simple specimen tests, that is: (1) increases in low-cycle fatigue strength for a given life are not commensurate with increases in yield strength, and (2) low-cycle fatigue life is closely related to total strain range and appears to be independent of both structural metal and strength level in the life range of 1000 to 30,000 cycles.